Chapter 11

Applications in medicine, biology, chemistry, and physical sciences

11.1 ▪ Medicine

11.1.1 ▪ Presentation of the domain

The type and number of observations that are available in medicine today are impressive (see also Section 11.4). In cardiology alone, we can cite electrocardiograms, MRI, CT scans, flow measurements with ultrasound, pressure measurement with catheters, and myocardium thickness measurement with piezoelectric sensors. The grand challenge is to use and combine these sources to solve inverse problems that will then lead to personalized medicine. DA in this field is novel, and many promising avenues remain to explore.

Wherever we encounter reaction-diffusion equations, there exists the possibility to use adjoint and DA approaches. This has been the case for studying tumor growth [Bresch et al., 2010; Colin et al., 2014] and cardiac electrophysiology (see below). This was also seen above (see Section 8.5) for the modeling of forest fires and in Chapter 2 in a theoretical context. Hemodynamics is another field for potential DA where we can either propose simple models of blood flow (see Section 11.3 on fluid dynamics) or also take into account the mechanics of arterial walls in a fluid–structure interaction model—see for example Perego et al. [2011], Bertoglio et al. [2012, 2013, 2014], Pant et al. [2014], and the website of the euHeart project (`http://www.euheart.eu`), where a lot of groundbreaking work was done.

11.1.2 ▪ Examples of DA problems in this context

11.1.2.1 ▪ Tumor growth

The mathematical modeling of cancer is aimed at understanding and then being able to predict the growth of a tumor. Just as important is the capacity of these models to thus simulate and reproduce the effects of anticancer therapies, be they chemotherapy or radiotherapy or any combination of these, by including their effects in the model. With the ever-increasing availability of medical imaging, a new era is opening up for better parameterization of these models in light of these images. This is precisely where inversion methods and DA can begin to provide hope for personalized therapeutic protocols.

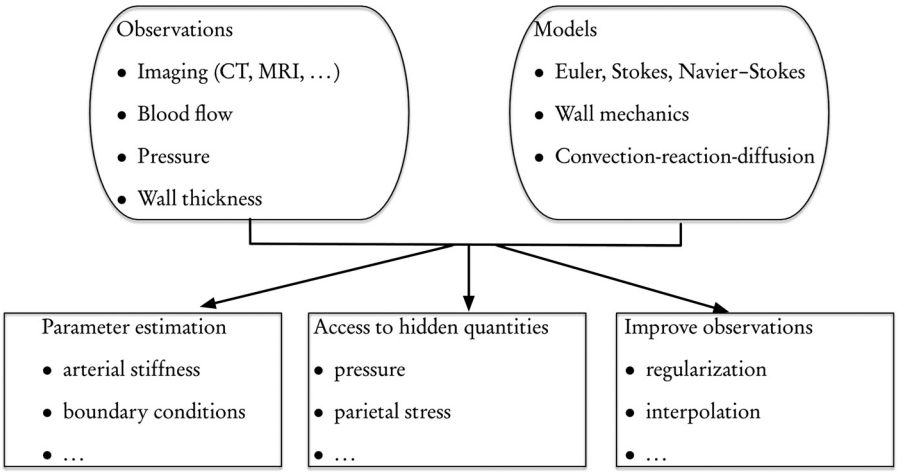

Figure 11.1. *Assimilation of medical data for the cardiovascular system (adapted from a presentation of J.-F. Gerbeau).*

The complete modeling of oncogenesis is considered to be out of reach, but there is no doubt that the coupling of simpler, PDE-based models with image sequences can provide helpful insight into the progression of the disease. In Lombardi et al. [2012], the case of lung metastases is studied.

Modeling of tumor growth has been described in Cristini and Lowengrub [2010]. In Lombardi et al. [2012] and Colin et al. [2014], inverse problems are formulated and solved for the identification of difficult to access parameters that lead to remarkably accurate predictions of tumor growth.

There are numerous perspectives in this domain, e.g., employing functional imaging (PET, flux, and diffusion MRI), use of biomarkers, and studies of placebo effects.

11.1.2.2 ▪ Hemodynamics

Understanding and modeling blood flow is a basic necessity for studying pathologies and estimating the effects of treatments in cardiology, e.g., stents, valves, etc. The physics of blood flow is in fact coupled with arterial wall movements, thus giving rise to fluid–structure interaction (FSI) problems. However, there is a hierarchy of models that can be applied to the problem, ranging from response functions up to full 3D PDEs [Formaggia et al., 2009]. In all cases, the need for estimating unknown parameters arises. With the deluge of measured data that is now available (see Figure 11.1), we are clearly in a position to formulate and solve DA and inverse problems for personalized medicine. In Bertoglio et al. [2014], the stiffness of the artery wall was estimated with the aid of a reduced-order unscented KF coupled with an FSI model.

Functional magnetic resonance imaging (fMRI) is based on studying the vascular response in the brain to neuronal activity and can be used to study mental activity. The ability to accurately model the evoked hemodynamic response to a neural event plays an important role in the analysis of fMRI data [Lindquist et al., 2008]. It is most commonly performed using blood oxygenation level–dependent (BOLD) contrast to study local changes in deoxyhemoglobin concentration in the brain. The primary goal of fMRI research is to use information provided by the BOLD signal to draw

conclusions about the underlying, unobserved neuronal activity. This response can be modeled at different levels, starting from relatively simple linear time-independent (LTI) response functions and moving up to full fluid dynamic modeling (see the following section). Once the models are defined, parameter estimation inverse problems can be formulated and solved by comparing with measured data (as seen above), usually from imaging—see for example Liu and Hu [2012].

11.1.2.3 ▪ Cardiac electrophysiology

The function of the heart is to pump blood through the circulatory system. To achieve this, the chambers (atria, ventricles) contract during the cardiac cycle. This contraction is triggered by an electrical impulse that takes the form of a wave propagating across the heart and depolarizing the cardiac muscular cells. An ECG (electrocardiogram) provides a noninvasive measurement of this electrophysiology. The Dutch doctor Willem Einthoven was awarded the Nobel Prize in Medicine in 1924 for the invention of the ECG.

The progression of the depolarization wave can be modeled by a reaction-diffusion equation, and the resulting numerical simulations can produce remarkably accurate synthetic ECGs [Boulakia et al., 2010].

The next step is electromechanical coupling—see Focus in Section 11.1.3—where the electrophysiology is coupled with a mechanical model of the heart's muscular contraction by the myocardium. Based on this, interesting electromechanical inverse problems can be formulated.

11.1.3 ▪ Focus: Electrocardiography inverse problem

This inverse problem involves the reconstruction of the heart's electrical activity from measurements of the body surface potential (as obtained by an ECG). A multiphysics approach is proposed in Corrado et al. [2015]. This approach combines a nudging or Luenberger observer for the mechanical state estimation with a reduced-order, unscented KF for the identification of the electrophysiological parameters—it is thus a *hybrid* DA method based on a joint gain filter. In fact, the mechanical measurements are shown to improve the identifiability of the electrical problem and produce an improved reconstruction of the electrical state. The computational challenge is huge: different meshes are used for the mechanics (18 000 elements), the electrics (540 000 elements), and the complete thorax (1.25 million elements); a master–slave coupling is used to transfer information between the electrical and mechanical solvers; uncertainties are taken into account; both mechanical and electrical measurements are used.

This model can now be coupled with real patient data, coming from ECG, tagged MRI, anatomy, and physiology. A patient workflow can be defined and thus provide a complete and personalized diagnostic, prevention, or pre- or post-operation planning and surveillance tool.

11.2 ▪ Systems biology

11.2.1 ▪ Presentation of the domain

Systems biology is based on the premise that it is not enough to understand how cellular components function to study whole cells or organisms. To predict a complete system's behavior, we need to consider the interactions between system components. This can be achieved, in the biological context (as well as in others—see for example

Section 11.3 below on fluid dynamics), by combining experimental techniques with computational methods and thus developing predictive models. Of course, with the arrival of the "-omics," in particular genomics and metabolomics, there is now an enormous amount of available observation data for this.

11.2.2 ▪ Examples of DA problems in this context

In the excellent review paper of Engl et al. [2009], they define two major classes of inverse problems for systems biology: (1) parameter identification based on the vast amount of available data, and (2) qualitative inverse modeling, which aims at reaching targeted dynamics. An example of the first class is to seek parameter values that stop growth of certain cell types and thus inhibit malignant growth. Another example that corresponds to class (2) is how to adjust circadian rhythms so that they respond more rapidly and smoothly to pacemaker calibration to counteract effects of jet lag.

Traditionally, chemical reaction networks are modeled by large systems of coupled ODEs that originate from Michaelis–Menten reaction kinetics [Wikipedia, 2016c]—see also Section 11.6. The dimension of these systems can be several thousands of equations and parameters. Parameter identification problems for these systems are solved by the classical data-mismatch approach using local (gradient-based) or global (stochastic) methods. The ill-posedness of the inverse problem is usually treated by the use of regularization techniques (see Chapters 1 and 2 and Engl et al. [1996]). The qualitative inverse problems are based on bifurcation diagrams that capture the direct relation between the cell physiology and the qualitative dynamics of the system under study. This is also used in chemical and electrical engineering problems and is related to what are known as "robust system" design techniques. The algorithms use gradient-based methods to place bifurcation points at desired locations.

11.3 ▪ Fluid dynamics

11.3.1 ▪ Presentation of the domain

Fluid dynamics covers a vast field of applications. These range from aerodynamics to meteorology, passing through experimental fluid mechanics and dynamics, going down to the level of blood-flow monitoring within the human body.

The application of DA methods to experimental fluid dynamics (EFD) has recently begun to be explored and can hopefully bridge gaps between EFD and computational fluid dynamics (CFD). Adjoint methods have been used for some time already to solve the inverse problem of aerodynamics for optimal shape design of airfoils and even complete airplanes. Another recent area of research combines fluid dynamics with image processing and is being applied to oceanographic and meteorological contexts.

11.3.2 ▪ Examples of DA problems in this context

11.3.2.1 ▪ Aerodynamics

The use of adjoint methods for optimal design in aerodynamics was initiated by Pironneau [1974]. The approach follows exactly the presentation in Chapter 2.

Since a wing is an apparatus for controlling the flow around an airplane, one can apply the theory of optimal control of PDEs to their design [Pironneau, 1974; Jameson, 1988; Giles and Duta, 2003]. This is based on the Euler equations for compressible flows and the Navier–Stokes equations for turbulent, incompressible flows from CFD

[Courant and Friedrichs, 1976; Batchelor, 2000; Kundu and Cohen, 2002]. A quadratic cost function is defined as

$$J = \frac{1}{2}\int_{\mathscr{B}} (p - p_t)^2 \, \mathrm{d}\mathscr{B},$$

where $\mathscr{B}$ is the surface shape of the airfoil, p is the fluid pressure field, and p_t is the target pressure distribution. The surface shape, after being suitably parameterized by a set of geometric design variables, is treated as the control function, which is varied to minimize J. A variation in the shape causes a variation in the pressure field and a subsequent variation in the cost function. Then, using the classical adjoint approach, we can formulate a gradient algorithm for optimizing the shape, exactly as was done in Chapter 2. To avoid a solution with a nonsmooth shape, Jameson [2006] proposed a weighted Sobolev gradient that enables the generation of a sequence of smooth shapes. This approach has been successfully applied to a large number of practical design problems, ranging from classical NACA airfoils to Boeing 747 wing fuselages [Vassberg and Jameson, 2002; Leoviriyakit and Jameson, 2004].

11.3.2.2 ▪ Experimental fluid dynamics

In a recent special issue, Suzuki [2015], the application of DA methods to EFD is explored. The motivation is to study the coupling of EFD with CFD. This coupling has, until now, been developed chiefly in the fields of geophysics, oceanography, and meteorology (as we have amply seen in previous chapters of this book). The idea is to introduce the variational and sequential methods that have been developed in these fields into the domain of fluid dynamics. This could help to overcome mutual weaknesses in EFD and CFD.

Measurements, and measurement devices, can characterize real-world flows, but they are often inadequate due to their limitation in time and space, their inaccuracy, and the fact that a measurement instrument can actually perturb the flow that we want to measure. These shortcomings have traditionally been dealt with by various interpolation and approximation techniques. But thanks to recent developments in CFD and the increasing capacity of HPC (high-performance computing), we are now able to simulate and reproduce real flows and correctly represent complex geometries, fine-scale flow structures, boundary and initial conditions, and even turbulent flows. Whereas the first two are well within the reach of CFD, the last two could greatly benefit from coupling with EFD.

In Hayase [2015], the different measurement methods and techniques are reviewed, interpolation methods are listed, and the integration of numerical simulation with flow measurements is discussed. This leads to the notion of a "hybrid wind tunnel," where simulation and measurement can be efficiently combined.

11.3.2.3 ▪ Coupled fluid dynamics with image analysis

The coupling of image sequences with fluid dynamics models by DA methods has been applied to geophysical flows and in EFD (see above). This has been particularly interesting for the understanding and the prediction of turbulent flows.

Sequences of satellite images furnish the possibility to follow scalar quantities, such as temperature, pressure, water vapor density, or phytoplankton density, that are transported by the flow. But the transport phenomena can be well described by PDEs that link the spatial and temporal variations of the field image to the unknown distribution

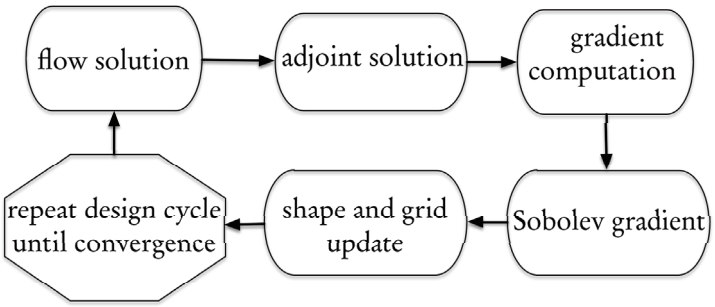

Figure 11.2. *Design cycle for aerodynamic shape optimization (adapted from Jameson [2006]).*

of flow velocities. We can thus constrain the observations by the model equations and proceed to assimilate the data.

A sequence of images inherently contains a large quantity of information, both spatial and temporal. The coupling with the Navier–Stokes equations can then be implemented by a variety of DA schemes and approaches. In Beyou et al. [2013], a weighted ETKF was used to assimilate ocean surface currents from images (observations) of sea surface temperatures. More recently, Yang et al. [2015] employed a hybrid ensemble-based 4D-Var scheme (4DEnVar—see Chapter 7) to assimilate a shallow-water model with simulated and real image sequences.

11.3.3 ▪ Focus: Optimal shape design in aerodynamics

Shape optimization [Delfour and Zolésio, 2001; Mohammadi and Pironneau, 2009] is a class of optimization problems where the modeling, optimization, or control variable is no longer a set of parameters or functions, but the shape or the structure of a geometric object. This is, in fact, an inverse problem. Adjoint methods are intensively used to compute gradients, and automatic differentiation (see Section 2.3.9) has often been employed. These gradient-based approaches are the only ones that make industrial problems tractable, and their use in aerodynamic design is now becoming widespread—see Figure 11.2.

In Jameson [2006], a continuous adjoint approach is applied to five concrete case studies: a transonic airfoil, a Boeing 747 planform, a super Boeing 747, a P51 racer, and a transonic executive jet. Results are obtained based on the Euler and Navier–Stokes equations. For the improvement of transonic performance, relatively small changes are needed in the wing cross-sections. To achieve truly optimal designs, the whole wing planform needs to be considered. The cost function must then include terms on both aerodynamics properties and overall structural weight. The functional takes the form

$$J = \alpha_1 C_D + \alpha_2 \frac{1}{2} \int_{\mathscr{B}} (p - p_t)^2 \, \mathrm{d}\mathscr{B} + \alpha_3 C_W,$$

where C_D is the drag coefficient and C_W is a dimensionless parameter of the wing weight. The three coefficients α_i permit the calculation of Pareto fronts for designs that have minimal weight for a given drag, or minimal drag for a given weight. The use of a smooth gradient—see also Schmidt et al. [2008], Schmidt [2010]—guarantees that the redesigned surface is always achievable.

11.4 ▪ Imaging and acoustics

11.4.1 ▪ Presentation of the domain

Imaging, in general, attempts to solve an inverse problem to characterize the medium (human body, machine part, etc.) from measurements taken on its surface. Usually a wave is emitted by a device, propagates through the medium, and is measured by a suitable sensor array. The waves can be elastic, acoustic, electromagnetic, or optic. Depending on the physical nature of the wave (basically its frequency and energy content), it will be able to penetrate different media at different resolutions.

11.4.2 ▪ Examples of DA problems in this context

11.4.2.1 ▪ Medical imaging

One of the most important successes in the field of inverse problems for imaging was the invention of an inversion algorithm for computed tomography (CT) by Cormack in 1963 [Wikipedia, 2015a] and its experimental demonstration by Hounsfield in 1973. These two received the Nobel Prize in Physiology or Medicine in 1979. Both CT and MRI are based on the theory of inverse problems. Recent work has addressed multimodal imaging, where two or more imaging techniques are combined to improve the accuracy and resolution of the inversion process [Ammari et al., 2011, 2012; Pulkkinen et al., 2014; Ammari et al., 2015].

11.4.2.2 ▪ Underwater acoustics

Similarly, in underwater acoustics [Jensen et al., 2011], there is an important emphasis on inverse problems. These inverse problems aim to elucidate properties of the sea water and the underlying sediment layers in the seabed from acoustic signals that are emitted by special acoustic arrays and measured on others, called hydrophones. Recently, adjoint methods have begun to be employed to this end [Asch et al., 2002; Hermand et al., 2006; Meyer et al., 2006]. Bayesian approaches have also been used [Dosso and Dettmer, 2011], but usually in a stationary setting—in fact the computations are generally performed in the frequency domain.

11.4.2.3 ▪ Geophysics and seismology

Of course, geophysical and seismic prospecting (see Chapter 10) is another context that has a lot in common with imaging and acoustics.

11.4.2.4 ▪ Image processing

Finally, a number of books are dedicated to inverse problems for image processing—see Colton and Kress [1998], Vogel [2002], and Kaipio and Somersalo [2005].

11.4.3 ▪ Focus: Inversion in underwater geoacoustics

Numerous inverse problems can be formulated in the field of underwater geoacoustics—see Figure 11.3. Among these we can single out the following:

1. ocean acoustic tomography (OAT), where we seek to reconstruct the sound-speed profile in the water layer, $c(z)$;

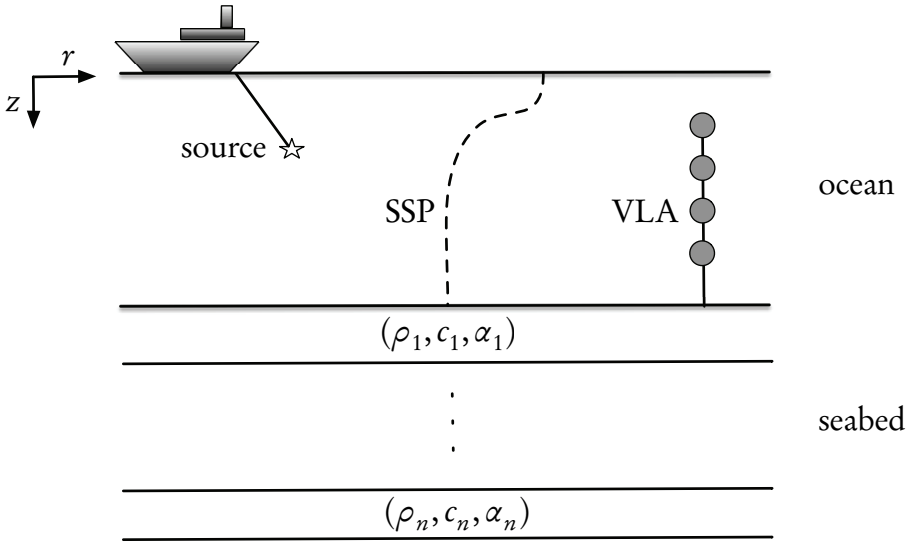

Figure 11.3. *Physical setup for a geoacoustics inverse problem. The ship tows an acoustic source, whose signal is measured on the vertical linear array (VLA). The acoustic signal propagates through the ocean, characterized by its sound-speed profile (SSP), $c(z)$, and penetrates into the n layers of sediments, characterized by their density ρ_i, sound speed c_i, and attenuation α_i. Note that the layer thicknesses can also be defined as parameters of the problem that are generally unknown.*

2. geoacoustic inversion (GI), where we seek to identify the sediment layer properties, $(\rho, c, \alpha)_m$, of layer m;

3. source or object detection;

4. buried object detection;

5. ocean impulse response, or Green's function reconstruction; and

6. tracking problems: sedimentation, currents, salinity, temperature, and other gradients.

According to D.M.F. Chapman, in Taroudakis and Makrakis [2001], "The goal of all geoacoustic inversions is to estimate environmental characteristics from measured acoustic field values, with the aid of a physically realistic computational acoustics model." A seismoacoustics model will clearly provide even better information for the inversions. In addition, ocean acoustics usually involves the measurement of a signal that propagates in a noisy environment. The array processing must take this into account. This gives rise to matched-field processing when the propagation medium is accounted for in the processing. In practice, although the acoustic measurements are obviously performed in the time domain, the processing is done in the frequency domain, thus requiring sophisticated Fourier transform techniques to have accurate spectral estimates. The use of spectral finite elements (SPECFEM) [Cristini and Komatitsch, 2012] will enable us to restore a full time domain signal processing capacity, thus leading (hopefully) to a much closer physical match with the recorded signals.

11.4.4 ▪ Focus: Photoacoustic tomography

The photoacoustic effect refers to the generation of acoustic waves by the absorption of optical energy [Fisher et al., 2007]. In photoacoustic imaging, energy absorption causes thermoelastic expansion of the tissue, which in turn leads to propagation of a pressure wave. This signal is measured by transducers distributed on the boundary of the organ, which is in turn used for imaging optical properties of the organ. Mathematically, the pressure, p, satisfies the wave equation

$$\frac{\partial^2 p}{\partial t^2}(x,t) - c^2 \Delta p(x,t) = 0, \quad x \in \Omega, \quad t \in]0,T[,$$

with the boundary condition

$$p(x,t) = 0 \quad \text{on } \partial\Omega \times]0,T[,$$

and the initial conditions

$$p(x,t)|_{t=0} = a\delta_{x=z} \quad \text{in } \Omega,$$

and

$$\partial_t p(x,t)|_{t=0} = 0 \quad \text{in } \Omega,$$

where a is the absorbed energy.

In Ammari et al. [2011], different imaging algorithms are used to reconstruct point obstacles. When only limited-view measurements are available, the coupling with an adjoint-based optimal control problem enables good reconstruction. It is shown that if one can accurately construct the geometric control, then one can perform imaging with the same resolution using limited-view as using full-view data, as can be seen in Figure 11.4.

11.5 ▪ Mechanics

11.5.1 ▪ Presentation of the domain

Mechanics is a field where a very large number of inverse problems exist. We can mention optimal design of mechanical structures (beams, trusses, plates), crack detection in materials, and parameter identification. Even the simplest mechanical system, made up of a mass, a spring, and a damper, gives rise to a number of inverse problems. The configuration of Figure 11.5 can be described by the linear dynamic state equation

$$M\ddot{\mathbf{u}} + C\dot{\mathbf{u}} + K\mathbf{u} = F,$$

with initial conditions

$$\mathbf{u}(0) = u_0, \quad \dot{\mathbf{u}}(0) = u_1.$$

Two classes of inverse problems can be defined:

1. Structural model updating, where for known $\mathbf{u}$ and F we seek to identify the system parameters, M, C, and K. This is also known as structural optimization.

2. Structural load updating, where for given $\mathbf{u}$, M, C, and K we seek the load, F.

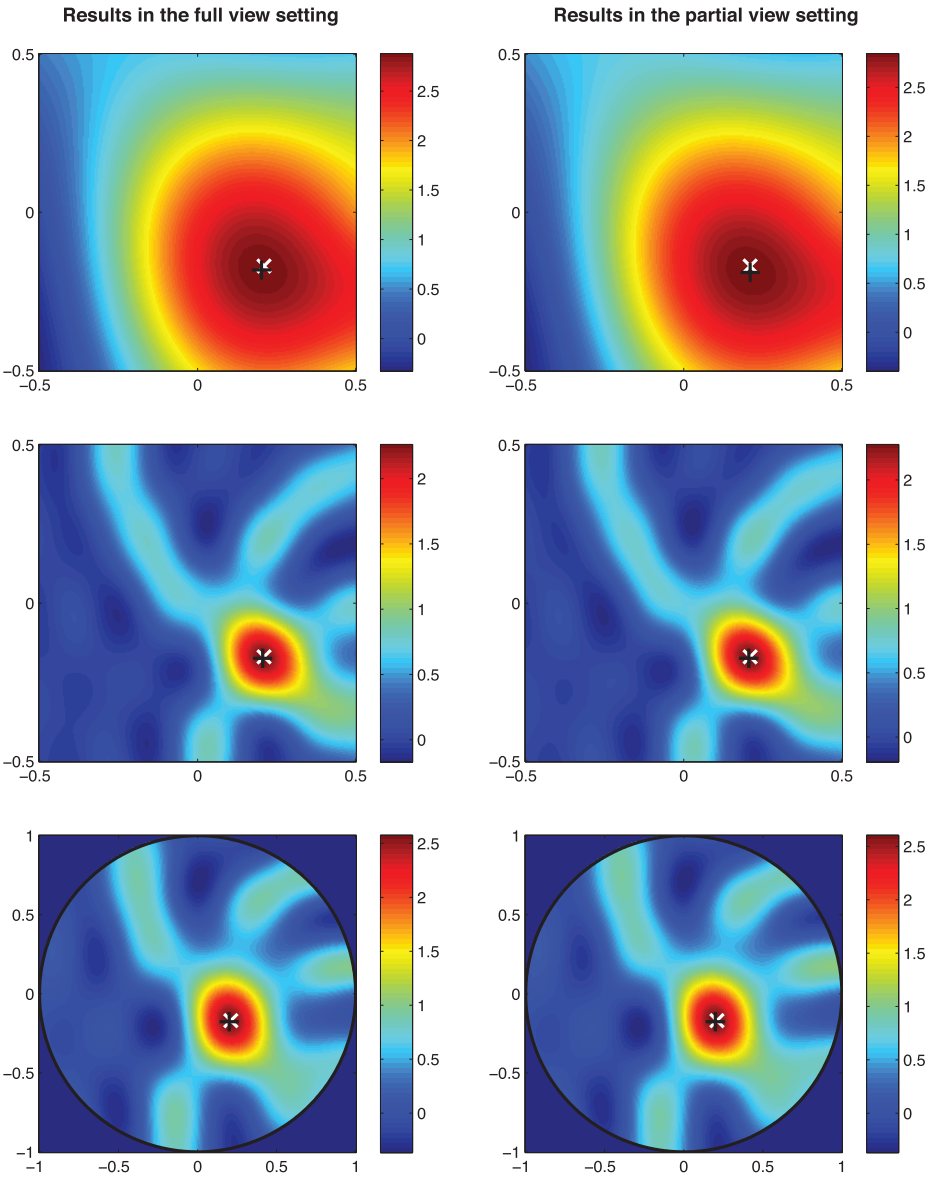

Figure 11.4. *Kirchhoff imaging algorithm results for source localization in square and circular geometries. The (black/white) x denotes the (numerical/theoretical) center of the source. Full- and limited-view results are essentially equivalent in their precision [Ammari et al., 2011].*

The theoretical background for these problems has already been treated in Chapter 2, Section 2.3.

A more complete setting can be found in Moireau et al. [2008] and Chapelle et al. [2009]. They describe PDE-based models where an extended Kalman filter (EKF) is coupled with a parameter estimation method to solve inverse problems in continuum mechanics. This approach was subsequently applied to cardiac biomechanics problems—see Section 11.1 above.

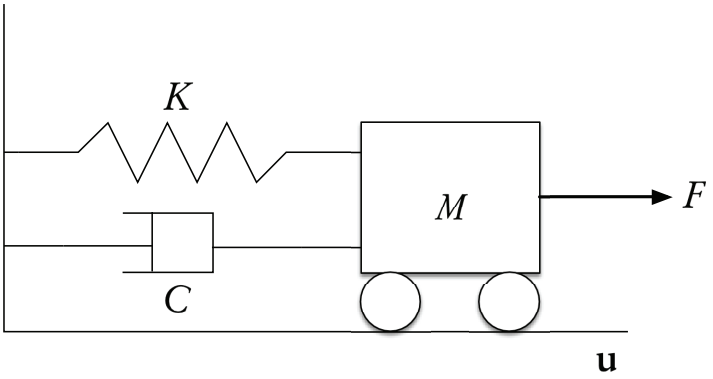

Figure 11.5. *A simple mechanical system, composed of a spring with stiffness K, a dashpot with coefficient C, and a mass M subject to a force F that produces a movement (displacement and velocity)* **u**.

11.5.2 ▪ Examples of DA problems in this context

The applications in mechanics are numerous. They range from heat-conduction problems in steel manufacturing [Engl and Kugler, 2005] to crack identification [Bonnet and Constantinescu, 2005] and biomechanics [Imperiale et al., 2013].

Many other mechanics-related applications can be found in the other sections of this part of the book, in particular, fluid mechanics (see Section 11.3), medicine (see Section 11.1), and geomechanics (see Section 10.1).

11.6 ▪ Chemistry and chemical processes

11.6.1 ▪ Presentation of the domain

Chemistry and chemical processes have already been encountered in Section 9.2 on Atmospheric Constituents and Section 11.2 on Systems Biology. Here we will describe a class of applications that are based on differential algebraic equations (DAEs) or PDEs.

Adjoint methods are widely used in the control and sensitivity analysis of chemical processes. This is the case for systems described by all three classes of equations: ODEs, DAEs, and PDEs.

11.6.2 ▪ Examples of DA problems in this context

11.6.2.1 ▪ Fermentation processes

In Merger et al. [2016], an adjoint approach is used to control a wine-fermentation process (see below) that is modeled by a system of parabolic PDEs. Beer fermentation has also been studied, but based on more classical reaction kinetics described by ODEs—see Ramirez and Maciejowski [2007].

11.6.2.2 ▪ Petroleum products

In Biegler [2007], a case study of low-density polyethylene (LDPE), used in the manufacture of plastic bags, squeeze bottles, and plastic films, is analyzed. The system is

composed of 130 ODEs and 500 DAEs. Gradients of the objective function with respect to the control coefficients and the model parameters are calculated either directly from the DAE sensitivity equations or by integrating the adjoint equations. This enables real-time optimization that can then be used as a decision-making aid. In the monograph of Biegler [2010], a lot of supplementary background material as well as additional applications can be found.

11.6.3 ▪ Focus: Wine fermentation process

Modeling of fermentation is important in food, chemical, and pharmaceutical production. For wine fermentation, if X is the yeast concentration and N, O, S, and E are the nitrogen, oxygen, sugar, and ethanol concentrations, respectively, then the reactions are given by

$$a_2N + a_3O + a_4S \xrightarrow{\mu_1} a_1X,$$
$$a_5S \xrightarrow{\mu_2} a_6E + a_7T,$$

where μ_1 and μ_2 are the reaction rates and $a_1,\ldots,a_7$ are the yield coefficients. The models that are usually used to describe this reaction system are systems of ODEs derived from classical reaction kinetics.

If space-dependent concentrations and temperature variations are taken into account, we obtain a system of six PDEs of reaction-diffusion type. For example, the equation for X (see Merger et al. [2016] for full details of the system) is

$$\frac{\partial X}{\partial t} - \sigma_1 \Delta X = +a_1\mu_1(X,N,O,S,T) - \Phi(E)X,$$

where Δ is the Laplacian operator and $\Phi(E)$ is a term that models the dying of the yeast population at the end of the fermentation process due to a toxic concentration of ethanol. Neumann boundary conditions are applied and initial concentrations are imposed at time zero. Diffusion-type PDEs have already been encountered numerous times in this book—see for example Sections 2.3 and 11.1.

To optimize the fermentation process, a cost function is defined in terms of an unknown control function, u, the applied temperature of the cooling/heating cycle. The gradient of the cost functional with respect to u is obtained from the adjoint equation, a backward reaction-diffusion equation, and the optimal control is then computed by a quasi-Newton BFGS (Broyden–Fletcher–Goldfarb–Shanno) algorithm [Press et al., 2007; Nocedal and Wright, 2006]. Numerical experiments have demonstrated the effectiveness of the proposed optimal control.